A Comparison of Three-node Two-way PLC Channel Models

Angie A. G. Liong *, Lenin Gopal *, Filbert H. Juwono *, Choo W. R. Chiong *, and Yue Rong †
* Department of Electrical and Computer Engineering, Curtin University Malaysia, 98009 Miri, Sarawak, Malaysia
†Department of Electrical and Computer Engineering, Curtin University, Perth WA 6845, Australia
Email: angie.liong@postgrad.curtin.edu.my, {lenin, filbert.hilman, raymond.ccw}@curtin.edu.my, y.rong@curtin.edu.au

***Abstract*—Two-way relay-based power-line communication (PLC) has been used in many smart grid applications. It is necessary to model the channel characteristics of such system in order to design a reliable communication link between premises and data centre. The channel transfer function (CTF) is preferred to be found using the bottom-up approach, as it represents the true topology of the PLC network. In this paper, we model a bottom-up multipath channel model for single relay two-way PLC channel based on transmission and reflection coefficients. We also compare the proposed model with the ABCD method and the voltage ratio approach (VRA) method. We show that the multipath model can well represent the two-way relay-based PLC channel.**

***Index Terms*—PLC, relay, channel model, CTF, ABCD matrix, VRA method.**

I. Introduction

The rapid growth of smart grid systems has made power-line communication (PLC) technology popular for data transmission indoor and outdoor [1]. It is because PLC uses the existing power-line infrastructure without installing new wires, thereby no additional cost is required. Smart grid needs two-way communication links to send information from premises to data centre and vice versa. To improve the signal quality, a relay can be employed. The use of relay increases the diversity gain to handle the challenging PLC channel.

Relay-based PLC systems can be well designed through the understanding of PLC channel characteristics, which can be obtained through channel modelling. In the literature, a number of research works on the PLC channel modelling have been discussed. In general, PLC channel models are grouped into top-down approach and bottom-up approach.

The top-down approach uses a set of parameters to describe the channel and behavior characteristics of PLC networks [2]. The parameter values are derived from statistical analysis based on measurement data. This approach can work in either time domain or frequency domain. However, it is hard to connect to the physical topology due to the difficulties in setting up large test loops with physical characteristics and configurations. A well-known top-down PLC model was proposed by Zimmermann and Dostert in [3]. The Zimmermann-Dostert PLC channel model is represented by the sum of multipath components where each multipath component consists of a weighting factor, an attenuation factor, and a delay coefficient. The weighting and attenuation factors are obtained from measurement data. Another top-down method was proposed by Tonello in [4].

On the other hand, the bottom-up approach is performed by implementing the transmission line (TL) theory to obtain the channel transfer function (CTF) using the network information [5]–[7]. The bottom-up approach is more preferred as it represents the topology of the power-line network. PLC channel modelling task can be difficult because of different topology of power networks and its harsh nature. Yet, many researchers were able to model the PLC channel. In this approach, the PLC transfer function was derived by using several means, such as the ABCD matrix [8], the S-parameter [9], the multiconductor transmission line (MTL) approach [10], [11], IIR-Filter [12], and the voltage ratio approach (VRA) in [13]. A comparison between the ABCD and VRA models has been discussed in [14].

A single relay PLC channel model with the ABCD method has been proposed in [15]. An extension of this model to two-way single relay PLC was discussed in [16]. The derivation of composite CTF of the single-relay and two-relay two-way PLC systems has been discussed in [17]. In this paper, we propose a bottom-up multipath channel model for single relay two-way PLC channel. This method is derived from the top-down Zimmermann-Dostert model with modification of the parameters to be a bottom-up model. The parameters are obtained from the transmission and reflection coefficients as given in [18]. The proposed model is then compared with the ABCD and VRA models.

The remaining of this paper is organised as follows. Section II discusses cable parameters to calculate the CTFs. In Section III, CTFs for the three PLC channel models are shown and derived. Numerical examples are given in Section IV to verify the result. Finally, the main conclusion of work is highlighted in Section V.

II. Cable Parameters

According to electromagnetic theory, the source energy must be guided to achieve an efficient point-to-point transmission of power and information. At high frequencies, the power cables, or so called transmission lines, guide the transverse electromagnetic (TEM) waves along them. In this paper, the power cables are the typical single-phase house wiring which are made up of stranded copper conductors with PVC insulation. The wires, i.e. live, neutral and earth are laid inside metal conduits that is placed inside the concrete wall.

The power cable is characterized by its type based on parameters and length. In a PLC transmission line, the paired live and neutral wires, are placed parallel in uniform distance. This transmission line is characterized by its characteristic impedance Z_0 and the propagation constant γ given by

$$Z_0(f) = \sqrt{\frac{R + j2\pi fL}{G + j2\pi fC}} \tag{1}$$

$$\gamma(f) = \sqrt{(R + j2\pi fL)(G + j2\pi fC)} \tag{2}$$

where R, L, C, G are the per-unit-length resistance (Ω/m), inductance (H/m), capacitance (F/m), and conductance (S/m), respectively. The per-unit-length inductance and capacitance

978-1-7281-8065-6/20/$31.00 ©2020 IEEE

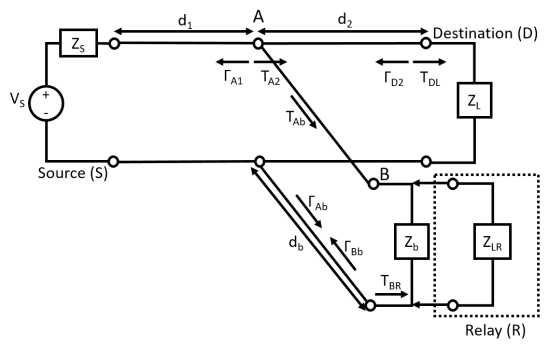

Fig. 1. Detailed topology of a PLC system for multipath model. The transmission and reflection factors shown here are only for the forward mode.

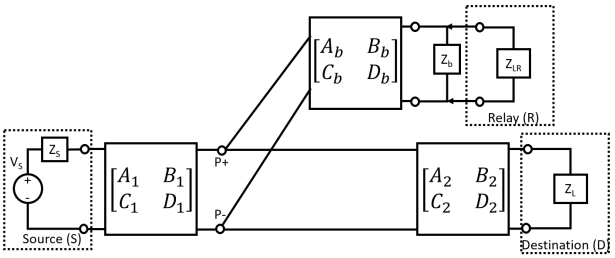

Fig. 2. Network layout of one-branch PLC channel model for the ABCD method.

are assumed constant for a given cable while the per-unit-length resistance and conductance are functions of frequency, given by $R = R_0\sqrt{f}$ and $G = G_0 \times \ell \times 2\pi f$, respectively, where ℓ is the cable loss and both R_0 and G_0 are constants [19].

III. Single Relay PLC Channel Modelling

In this paper, we focus on three types of channel models, i.e. the newly proposed multipath model, the ABCD method, and the VRA method. For simplicity, we use a single-relay PLC system model consisting of source (S), relay (R) and destination (D). The two-way PLC channel has two modes: forward mode and reverse mode. The forward mode refers to the mode when the signal is transmitted from S to D and the reverse mode refers to the mode when the signal is transmitted from D (which acts as a transmitter) to S (which acts as a receiver). We also assume that the length of each link is long enough so that there is no reflection from the far end. Each channel model is formulated as below.

We can infer from the description above that the source, relay, and destination nodes can act as either a transmitter or a receiver. Therefore, their inner impedance value during the transmitting mode will be different from the one in the receiving mode.

A. Proposed Multipath Model

The bottom-up multipath model proposed in [18] is shown in Fig. 1. Note that Z_S, Z_b, Z_{LR}, and Z_L are the load impedances at the source, branch, relay, and destination, respectively. We assume that Z_b is the frequency-dependent impedance given by [19]

$$Z_b = \frac{R'}{1 + jQ(\frac{\omega}{\omega_0} - \frac{\omega_0}{\omega})}, \tag{3}$$

where R', ω_0 and Q are the resistance at resonance, resonance angular frequency, and quality factor respectively [19].

The overall CTF of a relay-based PLC network in each mode is given by

$$H(f) = \sum_{i=1}^{N} g_i \alpha_i e^{-j2\pi f \tau_i}, \tag{4}$$

where g_i is the gain factor of the i-th path derived from the transmission (T) and reflection coefficients (Γ), $\alpha_i = e^{-\gamma d_i}$ is the attenuation factor for the i-th path, γ is given by (2), d_i is the length of the i-th path, $\tau_i = d_i\sqrt{\epsilon_r}/c_0$ is the delay of the i-th path, ϵ_r is the relative permeability of the cable material, c_0 is the speed of light, and N is the number of relay links. In this paper, we consider two relay links for each mode, i.e. S-D and S-R-D for forward mode and D-S and D-R-S for reverse mode. We will derive the CTF for each link and we will not find the overall CTF. Note that, without loss of generality, we do not consider reflected paths for each relay link.

1) CTF of S-D Path: The signal travels from S to the branch point A and then to D. As a result, the CTF is given by

$$H_{SD}(f) = g_{SD}\alpha_{SD}e^{-j2\pi f\tau_{SD}}, \tag{5}$$

where $\tau_{SD} = d_{SD}\sqrt{\epsilon_r}/c_0$, $d_{SD} = d_1 + d_2$, $\alpha_{SD} = e^{-\gamma d_{SD}}$, and $g_{SD} = T_{A2}T_{DL}$. Here, $T_{A2} = 1 + \Gamma_{A1}$ is the transmission coefficient from node A to line 2 and $T_{DL} = 1 + \Gamma_{D2}$ is the transmission coefficient from node D to the load. Note that we need to include T_{DL} as the load does not match the characteristic impedance of the power-line. The reflection coefficients are expressed as $\Gamma_{A1} = (Z_0/2 - Z_0)/(Z_0/2 + Z_0)$ and $\Gamma_{D2} = (Z_L - Z_0)/(Z_L + Z_0)$.

2) CTF of S-R-D Path: The CTF function for this path is given by

$$H_{SRD}(f) = g_{SRD}\alpha_{SRD}e^{-j2\pi f\tau_{SRD}} + g_{RD}\alpha_{RD}e^{-j2\pi f\tau_{RD}}, \tag{6}$$

where
$\tau_{SRD} = d_{SRD}\sqrt{\epsilon_r}/c_0$,
$\tau_{RD} = d_{RD}\sqrt{\epsilon_r}/c_0$,
$d_{SRD} = d_1 + 2d_b + d_2$,
$d_{RD} = d_b + d_2$,
$\alpha_{SRD} = e^{-\gamma d_{SRD}}$,
$\alpha_{RD} = e^{-\gamma d_{RD}}$,
$g_{SRD} = T_{Ab}\Gamma_{Bb}T_{A2}T_{DL}$,
$g_{RD} = T_{A2}T_{DL}$,
$\Gamma_{Ab} = \Gamma_{A2}$,
$\Gamma_{Bb} = (Z'_{LR} - Z_0)/(Z'_{LR} + Z_0)$.
and Z'_{LR} is the equivalent impedance of branch Z_b parallel to load impedance of the receiving relay node Z_{LR} which can be written as

$$Z'_{LR} = Z_b \parallel Z_{LR}. \tag{7}$$

The first term of (6) shows that the signal travels from S to the branch point A then to the relay point B. However, upon acceptance of the relay, part of the signal is reflected back to the branch and goes to point D. In addition, the second part of (6) shows that the relay transmits the signal to point D.

3) CTF of D-R-S Path: Similar to the S-R-D path, the CTF of the D-R-S path can be written as

$$H_{DRS}(f) = g_{DRS}\alpha_{DRS}e^{-j2\pi f\tau_{DRS}} + g_{RS}\alpha_{RS}e^{-j2\pi f\tau_{RS}}, \tag{8}$$

where $d_{DRS} = d_{SRD}$, $d_{RS} = d_{SR}$, $\tau_{DRS} = \tau_{SRD}$, $\tau_{RS} = \tau_{SR}$, $\alpha_{DRS} = \alpha_{SRD}$, $\alpha_{RS} = \alpha_{SR}$, $g_{DRS} = T_{Ab}\Gamma_{Bb}T_{A1}T_S$, $g_{RS} = T_{A1}T_S$, $T_{A1} = 1 + \Gamma_{A1}$, and $T_S = 1 + \Gamma_S$.

4) CTF of D-S Path: Using the same concept as the S-D path, we have the following CTF

$$H_{DS}(f) = g_{DS}\alpha_{DS}e^{-j2\pi f\tau_{DS}}, \tag{9}$$

where $g_{DS} = T_{A1}T_S$, $\Gamma_S = (Z_S - Z_0)/(Z_S + Z_0)$, $\tau_{DS} = d_{DS}\sqrt{\epsilon_r}/c_0$, $d_{DS} = d_{SD}$, and $\alpha_{DS} = e^{-\gamma d_{DS}}$.

B. ABCD Method

In order to get the ABCD matrix, Canate's hybrid point-to-point (P2P) channel model is used which consists of two segments and one branch terminated by a load impedance. Fig. 2 shows the network layout of one-branched PLC channel model used for this method. We assume the amplification factor $A_F = 1$. The CTFs can be derived as follows [16].

1) CTF of the direct path S to D: The ABCD matrix between S and D is given by

$$\begin{aligned}\Phi_{SD}^{(1)} &= \begin{bmatrix} A_{SD}^{(1)} & B_{SD}^{(1)} \\ C_{SD}^{(1)} & D_{SD}^{(1)} \end{bmatrix} \\ &= \begin{bmatrix} 1 & Z_S \\ 0 & 1 \end{bmatrix} \begin{bmatrix} A_1 & B_1 \\ C_1 & D_1 \end{bmatrix} \begin{bmatrix} 1 & 0 \\ \frac{1}{Z_{eqb,1}} & 1 \end{bmatrix} \begin{bmatrix} A_2 & B_2 \\ C_2 & D_2 \end{bmatrix},\end{aligned} \tag{10}$$

where, $Z_{eqb,1}$ is the equivalent input impedance of the relay branch as follows

$$Z_{eqb,1} = \frac{A_b Z'_{LR} + B_b}{C_b Z'_{LR} + D_b}. \tag{11}$$

where Z'_{LR} is the equivalent impedance of branch Z_b parallel to load impedance of the receiving relay node Z_{LR} which can be found using (7).

Therefore, the CTF of the direct path S to D is

$$H_{SD}^{(1)} = \frac{Z_L}{A_{SD}^{(1)}Z_L + B_{SD}^{(1)} + C_{SD}^{(1)}Z_L Z_S + D_{SD}^{(1)}Z_S}. \tag{12}$$

2) CTF of the path S to D through R: This part describes the connection between two paths, i.e. S to R and R to D. Looking at the first path, the ABCD matrix of path S to R is

$$\begin{aligned}\Phi_{SR}^{(1)} &= \begin{bmatrix} A_{SR}^{(1)} & B_{SR}^{(1)} \\ C_{SR}^{(1)} & D_{SR}^{(1)} \end{bmatrix} \\ &= \begin{bmatrix} 1 & Z_S \\ 0 & 1 \end{bmatrix} \begin{bmatrix} A_1 & B_1 \\ C_1 & D_1 \end{bmatrix} \begin{bmatrix} 1 & 0 \\ \frac{1}{Z_{eqb,2}} & 1 \end{bmatrix} \begin{bmatrix} A_b & B_b \\ C_b & D_b \end{bmatrix},\end{aligned} \tag{13}$$

where, $Z_{eqb,2}$ is the equivalent input impedance of destination node.

$$Z_{eqb,2} = \frac{A_2 Z_L + B_2}{C_2 Z_L + D_2}. \tag{14}$$

Thus, the CTF between S and R is

$$H_{SR}^{(1)} = \frac{Z'_{LR}}{A_{SR}^{(1)}Z'_{LR} + B_{SR}^{(1)} + C_{SR}^{(1)}Z'_{LR}Z_S + D_{SR}^{(1)}Z_S}, \tag{15}$$

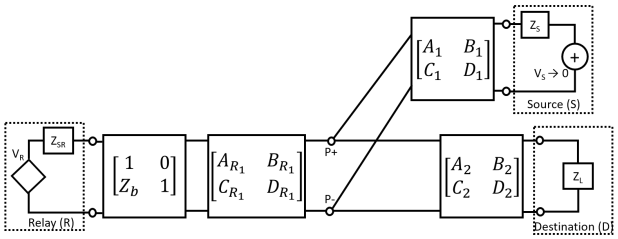

Fig. 3. Network layout of one-branch PLC channel model for the ABCD method (R to D)

At the second path, the ABCD matrix of path R to D is

$$\begin{aligned}\Phi_{RD}^{(2)} &= \begin{bmatrix} A_{RD}^{(2)} & B_{RD}^{(2)} \\ C_{RD}^{(2)} & D_{RD}^{(2)} \end{bmatrix} \\ &= \begin{bmatrix} 1 & 0 \\ Z_b & 1 \end{bmatrix} \begin{bmatrix} A_b & B_b \\ C_b & D_b \end{bmatrix} \begin{bmatrix} 1 & 0 \\ \frac{1}{Z_{eqb,3}} & 1 \end{bmatrix} \begin{bmatrix} A_2 & B_2 \\ C_2 & D_2 \end{bmatrix},\end{aligned} \tag{16}$$

where $Z_{eqb,3}$ is the equivalent input impedance of source node as shown below

$$Z_{eqb,3} = \frac{A_1 Z_S + B_1}{C_1 Z_S + D_1}. \tag{17}$$

Thus, the CTF of path from R to D is

$$H_{RD}^{(2)} = \frac{Z_L}{A_{RD}^{(2)}Z_L + B_{RD}^{(2)} + C_{DR}^{(2)}Z_{SR}Z_L + D_{DR}^{(2)}Z_{SR}}. \tag{18}$$

where Z_{SR} is the inner impedance of the relay node at the transmission mode which is shown in Fig. 3. Finally, the composite path gain of the entire S-R-D link is given by

$$H_{SRD} = H_{SR}^{(1)}A_F + H_{RD}^{(2)}. \tag{19}$$

3) CTF of the path D to S through R: Using similar method, link D to S through R consists of two paths, i.e. D-R path and R-S path. For the first path, the ABCD matrix from D to R is given by

$$\begin{aligned}\Phi_{DR}^{(1)} &= \begin{bmatrix} A_{DR}^{(1)} & B_{DR}^{(1)} \\ C_{DR}^{(1)} & D_{DR}^{(1)} \end{bmatrix} \\ &= \begin{bmatrix} A_2 & B_2 \\ C_2 & D_2 \end{bmatrix} \begin{bmatrix} 1 & 0 \\ \frac{1}{Z_{eqb,3}} & 1 \end{bmatrix} \begin{bmatrix} A_b & B_b \\ C_b & D_b \end{bmatrix},\end{aligned} \tag{20}$$

Thus, the CTF of the path D to R is

$$H_{DR}^{(1)} = \frac{Z'_{LR}}{A_{DR}^{(1)}Z'_{LR} + B_{DR}^{(1)} + C_{DR}^{(1)}Z'_{LR}Z_L + D_{DR}^{(1)}Z_L}. \tag{21}$$

At the second path, the ABCD matrix of path R to S is

$$\begin{aligned}\Phi_{RS}^{(2)} &= \begin{bmatrix} A_{RS}^{(2)} & B_{RS}^{(2)} \\ C_{RS}^{(2)} & D_{RS}^{(2)} \end{bmatrix} \\ &= \begin{bmatrix} 1 & 0 \\ Z_b & 1 \end{bmatrix} \begin{bmatrix} A_b & B_b \\ C_b & D_b \end{bmatrix} \begin{bmatrix} 1 & 0 \\ \frac{1}{Z_{eqb,2}} & 1 \end{bmatrix} \begin{bmatrix} A_1 & B_1 \\ C_1 & D_1 \end{bmatrix}.\end{aligned} \tag{22}$$

Thus, the CTF of the path R to S is given by

$$H_{RS}^{(2)} = \frac{Z_S}{A_{RS}^{(2)}Z_S + B_{RS}^{(2)} + C_{RS}^{(2)}Z_S Z_{SR} + D_{RS}^{(2)}Z_{SR}}, \tag{23}$$

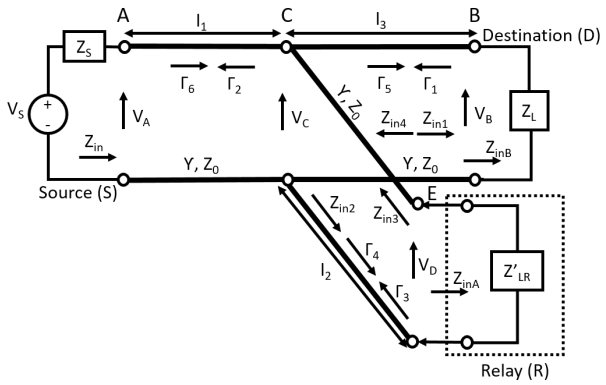

Fig. 4. Detailed topology of a PLC system for the VRA method.

Finally, the composite path gain of the entire D-R-S link can be expressed as

$$H_{DRS} = H_{DR}^{(1)} A_F + H_{RS}^{(2)}. \tag{24}$$

4) CTF of the direct path D to S: Therefore, the ABCD matrix between D and S is

$$\begin{aligned} \Phi_{DS}^{(1)} &= \begin{bmatrix} A_{DS}^{(1)} & B_{DS}^{(1)} \\ C_{DS}^{(1)} & D_{DS}^{(1)} \end{bmatrix} \\ &= \begin{bmatrix} A_2 & B_2 \\ C_2 & D_2 \end{bmatrix} \begin{bmatrix} 1 & 0 \\ \frac{1}{Z_{eqb,1}} & 1 \end{bmatrix} \begin{bmatrix} A_1 & B_1 \\ C_1 & D_1 \end{bmatrix}. \end{aligned} \tag{25}$$

Thus, the CTF of direct path D to S is

$$H_{DS}^{(1)} = \frac{Z_S}{A_{DS}^{(1)} Z_S + B_{DS}^{(1)} + C_{DS}^{(1)} Z_S Z_L + D_{DS}^{(1)} Z_L}. \tag{26}$$

C. VRA Method

Using VRA for the PLC network shown in Fig. 4, the CTFs of a PLC channel can be calculated as follows [9], [13], [14], [20].

1) CTF of the direct path S to D: The reflection coefficient of the end path, Γ_1 and reflection coefficient of Γ_2 from the tap point are

$$\Gamma_1 = \frac{Z_L - Z_0}{Z_L + Z_0}, \tag{27}$$

$$\Gamma_2 = \frac{Z_0/2 - Z_0}{Z_0/2 + Z_0}, \tag{28}$$

where Z_C is the equivalent impedance of Z_{in1} parallel to Z_{in2}.

Note that as we assume the length of each link is long enough, the input impedances can be approximated by $Z_{in} \approx Z_0$, $Z_{in1} \approx Z_0$, and $Z_{in2} \approx Z_0$. By applying shifting in reference planes [21],

$$\frac{V_B}{V_C} = \frac{(1+\Gamma_1)\, e^{-\gamma l_3}}{1+\Gamma_1 e^{-\gamma l_3}}, \tag{29}$$

$$\frac{V_C}{V_A} = \frac{(1+\Gamma_2)\, e^{-\gamma l_1}}{1+\Gamma_2 e^{-\gamma l_1}}, \tag{30}$$

$$\frac{V_A}{V_S} = \frac{Z_{in}}{Z_{in} + Z_S}. \tag{31}$$

Thus, the CTF of of the direct path S to D using the VRA method can be obtained as follows

$$H_{SD}(f) = \frac{V_A}{V_S} \times \frac{V_C}{V_A} \times \frac{V_B}{V_C}. \tag{32}$$

2) CTF of the path S to D through R: This session describes the connection between two paths, i.e. S to R and R to D. Looking at the first path, the CTF of the path S to R is given by

$$H_{SR}(f) = \frac{V_A}{V_S} \times \frac{V_C}{V_A} \times \frac{V_E}{V_C}, \tag{33}$$

where

$$\frac{V_E}{V_C} = \frac{(1+\Gamma_3)\, e^{-\gamma l_2}}{1+\Gamma_3 e^{-\gamma l_2}}, \tag{34}$$

The reflective coefficient of Γ_3 is

$$\Gamma_3 = \frac{Z'_{LR} - Z_0}{Z'_{LR} + Z_0}. \tag{35}$$

The CTF of the path R to D is given by

$$H_{RD}(f) = \frac{V_E}{V_R} \times \frac{V_C}{V_E} \times \frac{V_B}{V_C}, \tag{36}$$

where

$$\frac{V_E}{V_R} = \frac{Z_{inA}}{Z_{inA} + Z'_{LR}}, \tag{37}$$

$$\frac{V_C}{V_E} = \frac{(1+\Gamma_4)\, e^{-\gamma l_2}}{1+\Gamma_4 e^{-\gamma l_2}}. \tag{38}$$

Note that V_R is the source voltage when the relay acts as transmitter and $Z_{inA} \approx Z_0$.

The reflection coefficient of Γ_4 is

$$\Gamma_4 = \frac{Z_0/2 - Z_0}{Z_0/2 + Z_0}. \tag{39}$$

Finally, the composite path gain of the entire S-R-D link is given by

$$H_{SRD} = H_{SR} + H_{RD}. \tag{40}$$

3) CTF of the path D to S through R: Using similar method, link D to S through R consists of two paths, i.e. D-R path and R-S path. For the first path, the CTF of path D to R is

$$H_{DR}(f) = \frac{V_B}{V_L} \times \frac{V_C}{V_B} \times \frac{V_E}{V_C}, \tag{41}$$

where

$$\frac{V_B}{V_L} = \frac{Z_{inB}}{Z_{inB} + Z_L}, \tag{42}$$

$$\frac{V_C}{V_B} = \frac{(1+\Gamma_5)\, e^{-\gamma l_3}}{1+\Gamma_5 e^{-\gamma l_3}}. \tag{43}$$

Similarly, V_L is the source voltage when the destination acts as the transmitter and we have $Z_{inB} \approx Z_0$. The reflection coefficient of Γ_5 is

$$\Gamma_5 = \frac{Z_0/2 - Z_0}{Z_0/2 + Z_0}. \tag{44}$$

For the second path, the CTF of path R to S is given by

$$H_{RS}(f) = \frac{V_E}{V_R} \times \frac{V_C}{V_E} \times \frac{V_A}{V_C}, \tag{45}$$

where

$$\frac{V_A}{V_C} = \frac{(1+\Gamma_6)\, e^{-\gamma l_1}}{1+\Gamma_6 e^{-\gamma l_1}}. \tag{46}$$

The reflection coefficient of Γ_6 is

$$\Gamma_6 = \frac{Z_S - Z_0}{Z_S + Z_0}. \tag{47}$$

Lastly, the composite path gain of the entire D-R-S link is given by

$$H_{DRS} = H_{DR} + H_{RS}. \tag{48}$$

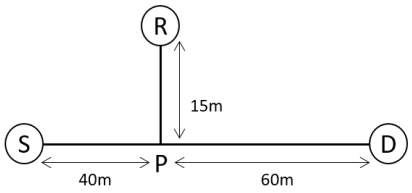

Fig. 5. Topology of a PLC channel

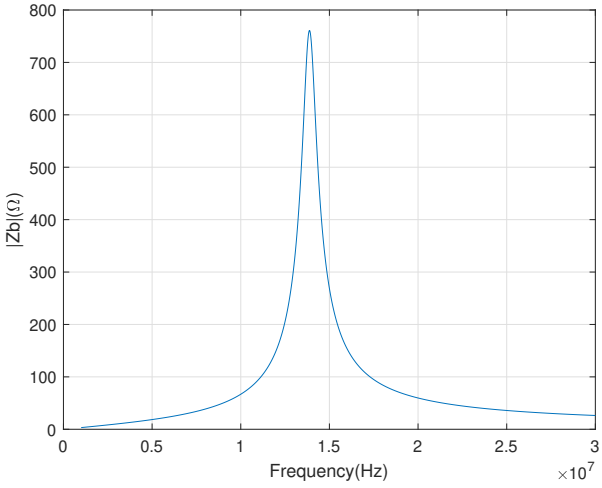

Fig. 6. Frequency response of Z_b

4) CTF of the direct path D to S: The CTF of direct path D to S is given by

$$H_{DS}(f) = \frac{V_B}{V_L} \times \frac{V_C}{V_B} \times \frac{V_A}{V_C}. \tag{49}$$

IV. Simulation Results

A simple three-node two-way topology used for simulations is shown in Fig. 5. As mentioned previously, we assume the same type of cable is used in each segment of the network. The cable parameters are as follows [19]: $R_0 = 6.25 \times 10^{-5}\Omega/m$, $L = 0.78 \times 10^{-6}H/m$, $C = 25 \times 10^{-12}F/m$, $G_0 = 42.5 \times 10^{-14}S/m$, $\ell = 5$, and $\epsilon_r = 1.73$. Moreover, R', $\omega_0/2\pi$, and Q of Z_b are drawn from uniform distributions on $\{200, 1800\}\Omega$, $\{2, 28\}MHz$, and $\{5, 25\}$, respectively [19]. A realization of the frequency response of Z_b is depicted in Fig. 6. We set the inner impedance in transmitting and receiving modes to be 50Ω and 150Ω, respectively.

Three different channel models are compared under four scenarios, i.e. S-D link, S-R-D link, D-R-S link, and D-S link. The simulation results of the four scenarios are compared and depicted in Figs. 7 to 10. It can be seen from the four figures that our proposed model does not fluctuate much, especially in the high frequency. In other words, it does not show much deep fades. This is because we do not include reflected paths in the relay links. The reflection results in more fluctuations. Interested readers may include the reflected paths. For example (refer to Fig. 5), reflected paths S-P-S-P-D path can be used for S-D link and S-R-P-R-P-D path (first term) and R-P-R-P-D path (second term) can be used for S-R-D link. However, these additional terms may have little effect on the CTF and can be neglected.

From Fig. 7, we notice that the CTFs of the ABCD model and the VRA model do not differ much and the multipath model

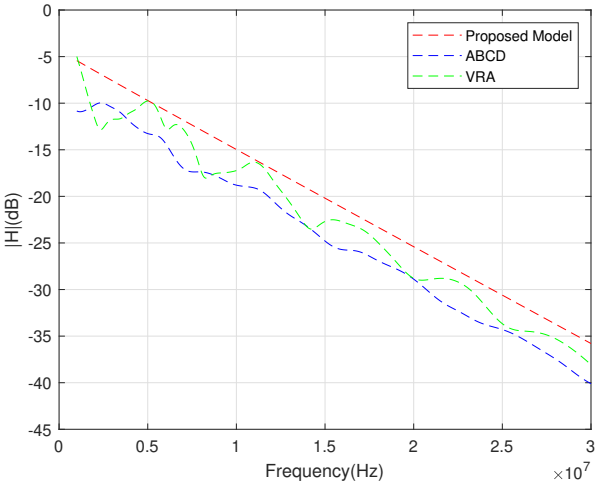

Fig. 7. Comparison of CTFs of the direct path S to D

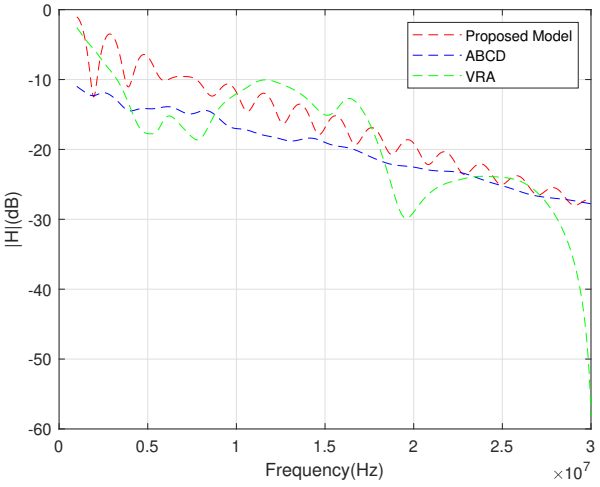

Fig. 8. Comparison of CTFs of the path S to D through R

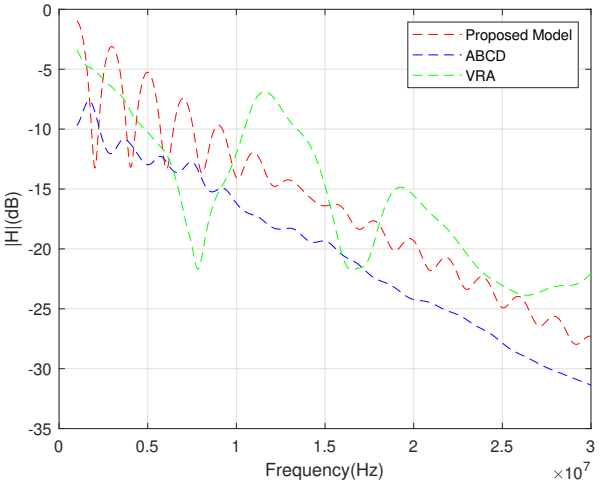

Fig. 9. Comparison of CTFs of the path D to S through R

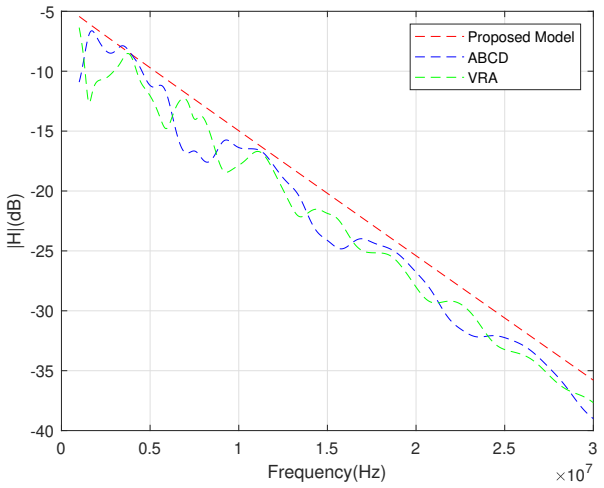

Fig. 10. Comparison of CTFs of the direct path D to S

gives the smallest attenuation. It can be seen from Fig. 8 that the three models are relatively equivalent, but the VRA model has high attenuation at high frequencies. On the other hand, it can be seen from Fig. 9 that the VRA model gives the lowest attenuation at high frequencies. From Fig. 10, it can be seen that the ABCD and VRA models give similar CTFs. In terms of attenuation at high frequencies, VRA model provides the largest attenuation for the SDR path and the smallest attenuation for the DRS path. For the SD and DS paths the three models are relatively comparable.

V. Conclusion

The bottom-up multipath channel model for a single relay two-way PLC channel has been proposed in the paper. This model has been derived on the modification of parameters of the top-down Zimmermann-Dostert model. We have also compared the proposed model of a single relay two-way PLC system with the ABCD and VRA models. It has been shown by simulations that the proposed model does not have much fluctuations/deep fades. It can also be seen that, for the direct paths, the three models show similar profile. On the other hand, for the SRD path at high frequencies, it has been observed that our proposed model has similar attenuation to the ABCD model. Finally, for the DRS path, our proposed model has better attenuation than the ABCD model at high frequencies.

Acknowledgment

This work was supported by Fundamental Research Grant Scheme (FRGS) from Ministry of Higher Education Malaysia under FRGS/1/2016/TK04/CURTIN/02/1.

References

[1] H. C. Ferreira, L. Lampe, J. Newbury, and T. G. Swart, *Power line communications: Theory and applications for narrowband and broadband communications over power lines*. Chichester, UK: Wiley, 2010.

[2] X. Zhao, H. Zhang, W. Lu, and L. Li, "Approach for modelling of broadband low-voltage PLC channels using graph theory," *IET Commun.*, vol. 12, no. 13, pp. 1524–1530, 2018.

[3] M. Zimmermann and K. Dostert, "A multipath model for the powerline channel," *IEEE Trans. Commun.*, vol. 50, no. 4, pp. 553–559, 2002.

[4] A. M. Tonello, F. Versolatto, B. Bejar, and S. Zazo, "A fitting algorithm for random modeling the PLC channel," *IEEE Trans. Power Del.*, vol. 27, no. 3, pp. 1477–1484, 2012.

[5] J. Anatory, N. Theethayi, R. Thottappillil, M. M. Kissaka, and N. H. Mvungi, "An experimental validation for broadband power-line communication (BPLC) model," *IEEE Trans. Power Del.*, vol. 23, no. 3, pp. 1380–1383, 2008.

[6] J. Anatory, N. Theethayi, and R. Thottappillil, "Power-line communication channel model for interconnected networks—part I: Two-conductor system," *IEEE Trans. Power Del.*, vol. 24, no. 1, pp. 118–123, 2009.

[7] A. M. Tonello and F. Versolatto, "Bottom-up statistical PLC channel modeling—part I: Random topology model and efficient transfer function computation," *IEEE Trans. Power Del.*, vol. 26, no. 2, pp. 891–898, 2011.

[8] T. Esmailian, F. Kschischang, and P. Gulak, "In-building power lines as high-speed communication channels: Channel characterization and a test channel ensemble," *Int. J. Commun. Systems*, vol. 16, pp. 381–400, Jun 2003.

[9] H. Meng, S. Chen, Y. L. Guan, C. L. Law, P. L. So, E. Gunawan, and T. T. Lie, "Modeling of transfer characteristics for the broadband power line communication channel," *IEEE Trans. Power Del.*, vol. 19, no. 3, pp. 1057–1064, 2004.

[10] S. Galli and T. Banwell, "A novel approach to the modeling of the indoor power line channel-part II: Transfer function and its properties," *IEEE Trans. Power Del.*, vol. 20, no. 3, pp. 1869–1878, 2005.

[11] J. Anatory, M. M. Kissaka, and N. H. Mvungi, "Channel model for broadband power-line communication," *IEEE Trans. Power Del.*, vol. 22, no. 1, pp. 135–141, 2007.

[12] G. Moreno-Rodriguez and L. T. Berger, "An IIR-filter approach to time variant PLC-channel modelling," in *Proc. IEEE Int. Symp. Power Line Commun. Appl. (ISPLC)*, Jeju City, South Korea, 2008, pp. 87–92.

[13] A. M. Tonello and T. Zheng, "Bottom-up transfer function generator for broadband plc statistical channel modeling," in *2009 IEEE International Symposium on Power Line Communications and Its Applications*, Dresden, Germany, 2009, pp. 7–12.

[14] A. Aloui, O. Ben Rhouma, and C. Rebai, "Comparison of different channel modeling techniques used in NB-PLC systems," in *2018 Int. Conf. Adv. Systems and Electric Technol. (ICASET)*, Hammamet, Tunisia, 2018, pp. 125–131.

[15] X. Wu and Y. Rong, "Channel model proposal for indoor relay–assisted power line communications," *IET Commun.*, vol. 12, no. 10, p. 1236–1244, 2015.

[16] A. A. G. Liong, L. Gopal, F. H. Juwono, C. W. R. Chiong, and Y. Rong, "A channel model for three-node two-way relay-aided PLC systems," in *Proc. IEEE Int. Conf. on Signal Image Process. Appl. (ICSIPA)*, Kuala Lumpur, Malaysia, 2019, pp. 52–57.

[17] A. A. G. Liong, L. Gopal, F. H. Juwono, C. W. R. Chiong, and Y. Rong, "Channel characteristics comparison of single-relay and two-relay two-way PLC systems," in *IEEE Int. Conf. Comp. Commun. Netw. Technol. (ICCCNT)*, Kharagpur, West Bengal, India, 2020.

[18] B. Adebisi, A. Khalid, Y. Tsado, and B. Honary, "Narrowband PLC channel modelling for smart grid applications," in *9th Int. Symp. Commun. Syst., Netw. Digital Signal Process. (CSNDSP)*, Manchester, UK, 2014, pp. 67–72.

[19] F. J. Canete, J. A. Cortes, L. Diez, and J. T. Entrambasaguas, "A channel model proposal for indoor power line communications," *IEEE Commun. Mag.*, vol. 49, no. 12, p. 166–174, 2011.

[20] S. Souissi, O. B. Rhouma, and C. Rebai, "Bottom-up approach for narrowband powerline channel modeling," in *2013 IEEE Global Commun. Conf. (GLOBECOM)*, Atlanta, GA, USA, 2013, pp. 2987–2992.

[21] D. Weston, *Electromagnetic compatibility: Principles and application*. CRC Press, 2001, vol. 4.